Supporting Information

Table S1. *Ionic conductivity and density of cell setups from* Figure 2.

Samples	Ionic Conductivity, mS cm^{-1} (at 100 MPa)	Density, g cm^{-3} (at 300 MPa)
Cell setup A	1.4	1.49 (theoretical value is 1.64)*
Cell setup B	0.9	2.42 (theoretical value is 2.6)**
Cell setup C	0.6	2.38
Cell setup D	0.8	2.28
Cell setup E	0.8	2.06
Cell setup F	1.5	1.75

Note: * [1] A. Tron, A. Paolella, A. Beutl, New insights of infiltration process of argyrodite Li_6PS_5Cl solid electrolyte into conventional lithium-ion electrodes for solid-state batteries, Batteries 9 (10) (2023) 503.

** [2] E. van der Maas, W. Zhao, Z. Cheng, T. Famprikis, M. Thijs, S.R. Parnell, S. Ganapathy, M. Wagemaker, Investigation of structure, ionic conductivity, and electrochemical stability of halogen substitution in solid-state ion conductor $Li_3YBr_xCl_{6-x}$, J. Phys. Chem. C 127, 1 (2023) 125–132.

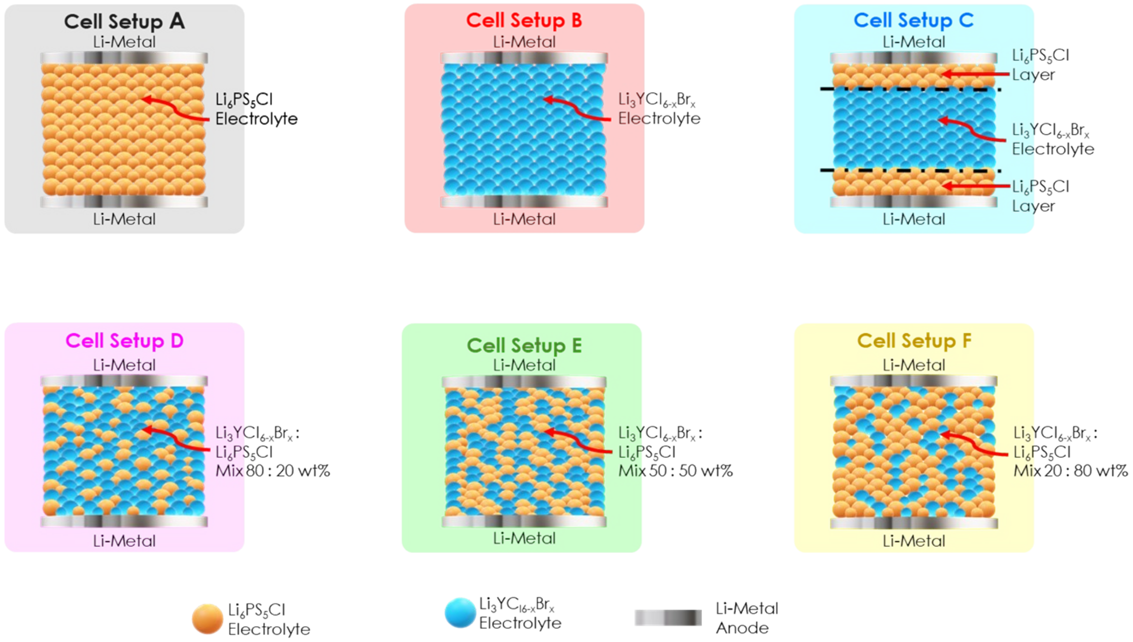

Figure S1. *Schematic of the different cell setups with different solid electrolyte combinations and lithium metal anode with the mixed electronic and ionic interface between lithium metal anode and halide and sulfide electrolytes. Note: anode | separator | anode for dry pellets: Cell setup A: Li | LPSC | Li; Cell setup B: Li | LYCB | Li; Cell setup C: Li | LPSC layer | LYCB | LPSC layer | Li; Cell setup D: Li | LYCB : LPSC (80 : 20 wt%) | Li; Cell setup E: Li | LYCB : LPSC (50 : 50 wt%) | Li; Cell setup F: Li | LYCB : LPSC (20 : 80 wt%) | Li.*

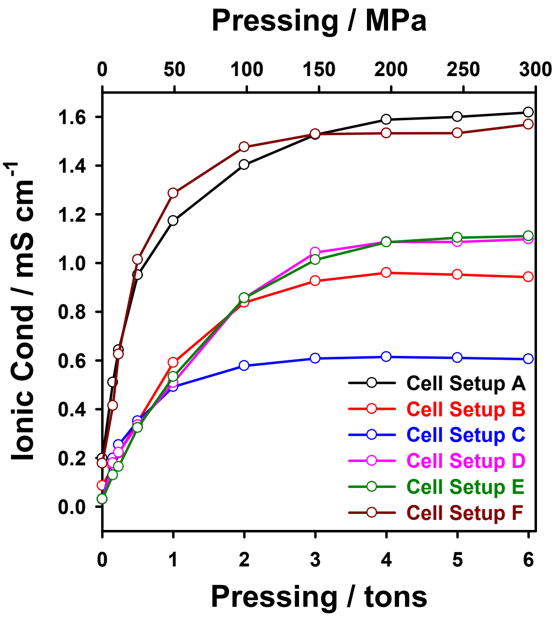

Figure S2. *Ionic conductivity of different cell setups with different solid electrolyte combinations and stainless steel (SS) electrode. Note: SS | separator | SS for dry pellets: Cell setup A: SS | LPSC | SS; Cell setup B: SS | LYCB | SS; Cell setup C: SS | LPSC layer | LYCB | LPSC layer | SS; Cell setup D: SS | LYCB : LPSC (80 : 20 wt%) | SS; Cell setup E: SS | LYCB : LPSC (50 : 50 wt%) | SS; Cell setup F: SS | LYCB : LPSC (20 : 80 wt%) | SS.*

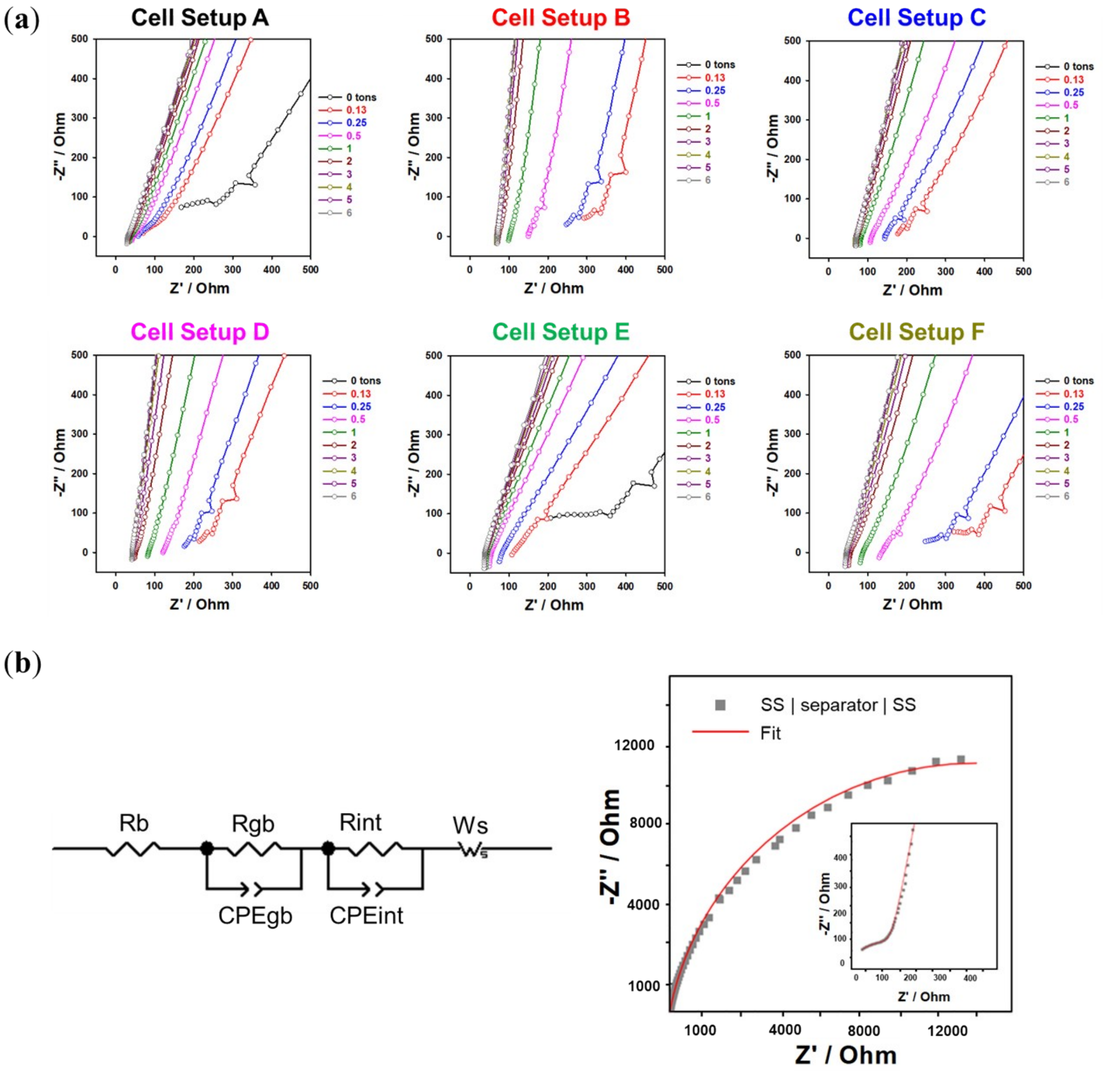

Figure S3. *(a) Nyquist plots of different cell setups with different solid electrolyte combinations and stainless steel (SS) electrodes. Note: SS | separator | SS for dry pellets: Cell setup A: SS | LPSC | SS; Cell setup B: SS | LYCB | SS; Cell setup C: SS | LPSC layer | LYCB | LPSC layer | SS; Cell setup D: SS | LYCB : LPSC (80 : 20 wt%) | SS; Cell setup E: SS | LYCB : LPSC (50 : 50 wt%) | SS; Cell setup F: SS | LYCB : LPSC (20 : 80 wt%) | SS. (b) Equivalent circuit and Nyquist plot with fitted curves (for example).*

Ionic conductivity measurements: Electrochemical impedance spectroscopy (EIS) measurements were performed in Potentiostatic EIS (PEIS) mode with a frequency range from 2 MHz to 10 Hz and a voltage amplitude of 10 mV amplitude. This approach was employed to evaluate the bulk ionic conductivity of both pristine and blended electrolytes in symmetric cells using stainless steel (SS) blocking electrodes (e.g., SS | Cell Setup | SS). The cells were tested at pressures ranging from 0 and 300 MPa in order to investigate the pressure-dependence behavior of the conductivity. The ionic conductivity of the electrolytes was then determined using specific equation 1 and the experimental setup is shown in Figure S3b. The measurements are performed at 25ºC, and the resulting data are analyzed using an equivalent circuit model via the ZView software package. The model consists of the following components: (Rb), (RgbCPEgb), (RintCPEint), and (Ws), where Rb represents the bulk resistance, Rgb and Rint correspond to the resistances associated with the grain boundary and electrode-electrolyte interface, respectively, and Ws denotes the Warburg element. The CPE terms (CPEgb and CPEint) refer to constant phase elements. The ionic conductivity (σ) of the Cell Setups is determined from Equation (1):

$$\sigma = \frac{l}{\left(\left(R_b + R_{gb}\right) \times A\right)} \quad \text{Equation (1)}$$

where l and A are the thickness and cross-sectional area of the solid electrolyte, respectively.

Table S2. *Obtained overpotential from plating and stripping process (CCD) of cell setups from* (Figure 4a).

Samples	Cycles / Overpotential mV							
	C/100	C/50	C/20	C/10	C/5	C/2	1C	2C
Cell setup A	2.3 / -2.8	4.6 / -5.0	11 / -11	20 / -22	34 / -44	32 / -144*	25 / -60*	27 / -66*
Cell setup B	11 / -11	14 / -14	21 / -19	44 / -44	96 / 121	292 / -323	605 / -600*	1000 / -1000*
Cell setup C	3.4 / -3.6	7.2 / -7.7	22 / -19	33 / -34	68 / -67	147 / -151*	197 / -174*	406 / -808*
Cell setup D	3.4 / -3.4	6.8 / -7.1	19 / -18	51 / -44	114 / -99	280 / -262	564 / -533	1221 / -1226*
Cell setup E	8 / -7	10 / -9	15 / -13	28 / -26	42 / -39	74 / -78*	106 / -115*	154 / -140*
Cell setup F	1 / -1	2 / -2	5.5 / -5.8	11 / -11	22 / -22	22 / -50*	10 / -35*	10 / -14*

Note: *short circuit for

- Cell Setup A at C/2;
- Cell Setup B at 1C;
- Cell Setup C at C/2;
- Cell Setup D at 2C;
- Cell Setup E at C/2;
- Cell Setup F at C/2.

Table S3. *Obtained overpotential from plating and stripping process (long cycle) of cell setups from* (Figure 4b).

Samples	Cycles / Overpotential mV						
	1st	5th	10th	20th	30th	40th	50th
Cell setup A	4 / -4	5 / -5	5 / -5	6 / -6	6 / -6	6 / -6	6 / -6
Cell setup B	11 / -16	25 / -29	26 / -30	32 / -38	38 / -39	39 / -40	47 / -50
Cell setup C	8 / -8	8 / -8	9 / -9	9 / -9	9 / -9	10 / -10	10 / -10
Cell setup D	8 / -9	15 / -15	20 / -20	22 / -22	24 / -23	27 / -25	33 / -30
Cell setup E	5 / -5	8 / -6	9 / -7	11 / -10	12 / -11	15 / -13	15 / -13
Cell setup F	4 / -4	5 / -5	5 / -5	6 / -6	6 / -6	6 / -6	6 / -6

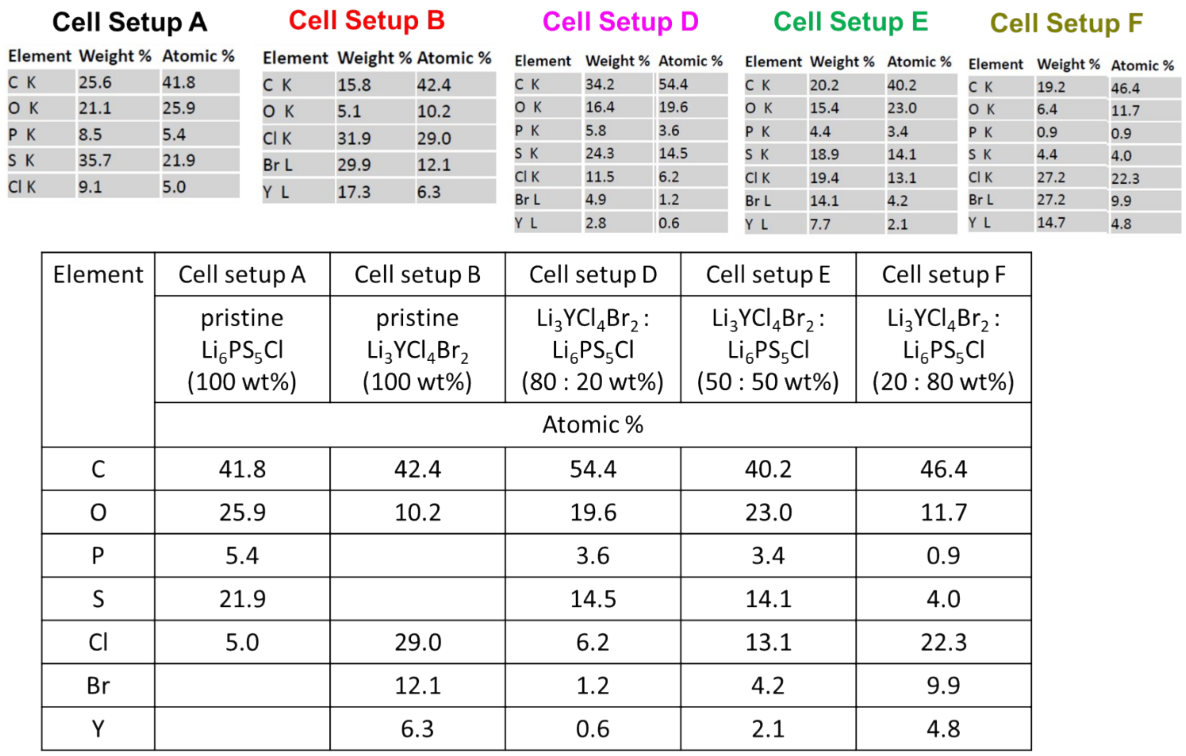

Cell Setup A

Element	Weight %	Atomic %
C K	25.6	41.8
O K	21.1	25.9
P K	8.5	5.4
S K	35.7	21.9
Cl K	9.1	5.0

Cell Setup B

Element	Weight %	Atomic %
C K	15.8	42.4
O K	5.1	10.2
Cl K	31.9	29.0
Br L	29.9	12.1
Y L	17.3	6.3

Cell Setup D

Element	Weight %	Atomic %
C K	34.2	54.4
O K	16.4	19.6
P K	5.8	3.6
S K	24.3	14.5
Cl K	11.5	6.2
Br L	4.9	1.2
Y L	2.8	0.6

Cell Setup E

Element	Weight %	Atomic %
C K	20.2	40.2
O K	15.4	23.0
P K	4.4	3.4
S K	18.9	14.1
Cl K	19.4	13.1
Br L	14.1	4.2
Y L	7.7	2.1

Cell Setup F

Element	Weight %	Atomic %
C K	19.2	46.4
O K	6.4	11.7
P K	0.9	0.9
S K	4.4	4.0
Cl K	27.2	22.3
Br L	27.2	9.9
Y L	14.7	4.8

Element	Cell setup A	Cell setup B	Cell setup D	Cell setup E	Cell setup F
	pristine Li_6PS_5Cl (100 wt%)	pristine $Li_3YCl_4Br_2$ (100 wt%)	$Li_3YCl_4Br_2$: Li_6PS_5Cl (80 : 20 wt%)	$Li_3YCl_4Br_2$: Li_6PS_5Cl (50 : 50 wt%)	$Li_3YCl_4Br_2$: Li_6PS_5Cl (20 : 80 wt%)
	Atomic %				
C	41.8	42.4	54.4	40.2	46.4
O	25.9	10.2	19.6	23.0	11.7
P	5.4		3.6	3.4	0.9
S	21.9		14.5	14.1	4.0
Cl	5.0	29.0	6.2	13.1	22.3
Br		12.1	1.2	4.2	9.9
Y		6.3	0.6	2.1	4.8

Figure S4. *EDS analysis of cell setups from* Figure 2.

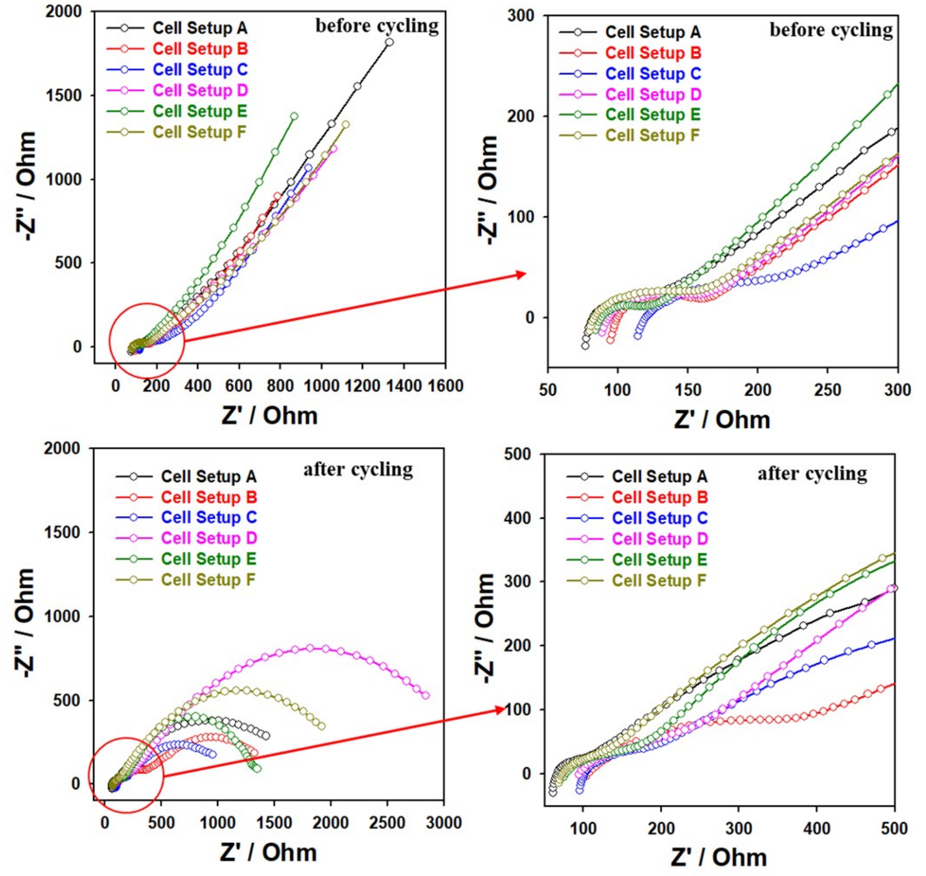

Figure S5. *Nyquist plots of cell setups from* Figure 5 *before (top) and after (bottom) cycling.*

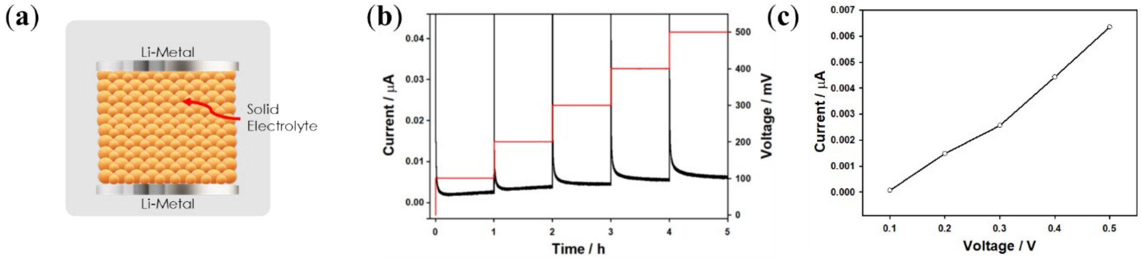

Figure S6. (a) *A schematic illustration of cell with stainless steel (SS) electrodes as the lithium-ion blocking cell, (b) Current and potential profile during electrical conductivity measurements of a SS|Cell setup|SS cell (left), and (c) the mean current was further plotted vs. the applied potential to determine the electric resistance and enable the calculation of the electronic conductivity (right).*

Electronic conductivity of dry pellets: A modified method based on a method reported in [3,4,5] was used to measure the value of the electronic conductivity. The electronic conductivity of the solid electrolytes (SE) was measured using stepwise changeable voltages in the range of 100 to 500 mV with 100 mV steps in the stainless steel (SS) blocking electrode/SE/blocking electrode cell. To follow the current responses in the cell, the cell voltage was held for 1 hour at each step. An exponential function was used to determine the dependence of the relaxation. The ionic component of the conductivity was responsible for the rapid current decrease (exponential parts of the function) that occurred in the cell during the first 100 seconds. The electronic conductivity was responsible for the residual current. The electronic conductivity of the solid electrolyte was measured from the slope of the voltammetric curve.

References:

[3] F. Vereda, R.B. Goldner, T.E. Haas, P. Zerigian, Rapidly grown IBAD LiPON films with high Li-ion conductivity and electrochemical stability, Electrochem. Solid-State Lett. 5 (2002) A239–A241.

[4] M. Menetrier, A. Lavasseur, P. Hagenmuller, Electrochemical properties of B_2S_3−Li_2S−LiI vitreous electrolytes, J. Electrochem. Soc. 131 (1984) 1971–1973.

[5] A. Tron, A. Nosenko, Y.D. Park, J. Mun, Synthesis of the solid electrolyte Li_2O–LiF–P_2O_5 and its application for lithium-ion batteries, Solid State Ion. 308 (2017) 40–45.

Table S4. *Obtained charge and discharge specific capacity values of cell setups from* (Figure 5).

Samples	Charge and Discharge specific capacity, mAh g^{-1}			
	1st Charge	1st Discharge	2nd Charge	2nd Discharge
Cell setup A	152	108	115	107
Cell setup B	196	150	152	149
Cell setup C	195	149	150	146
Cell setup D	184	134	129	127
Cell setup E	163	125	121	116
Cell setup F	176	130	127	126

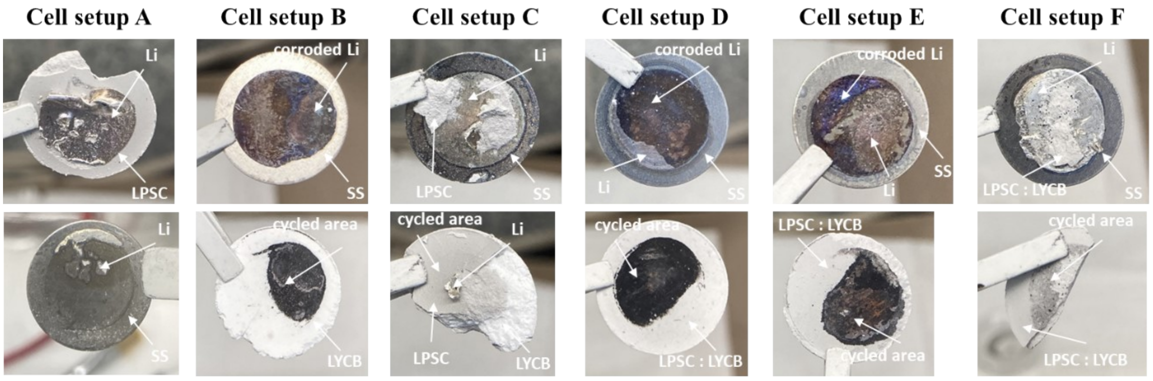

Figure S7. *Photos of Cell Setup pellets and lithium metal anodes after cycling (Figure 5a).*

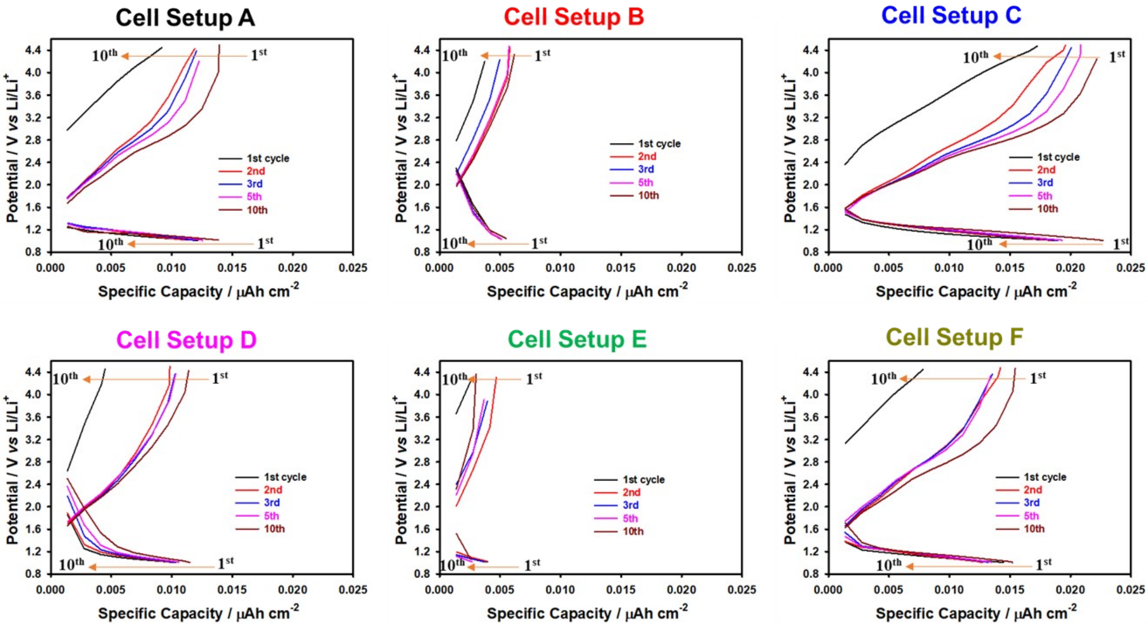

Figure S8. *The specific capacity of the Cell setups in cell configuration of SS|Cell setup|Li cell at the 50 µA cm^{-2} in the potential range of 1.0–4.3 V (vs. Li/Li^{+}). Note: anode | separator | current collector: Cell setup A: Li | LPSC | SS; Cell setup B: Li | LYCB | SS; Cell setup C: Li | LPSC | LYCB | SS; Cell setup D: Li | LYCB : LPSC (80 : 20 wt%) | SS; Cell setup E: Li | LYCB : LPSC (50 : 50 wt%) | SS; Cell setup F: Li | LYCB : LPSC (20 : 80 wt%) | SS.*

Electrochemical measurements: Galvanostatic cycling with potential limitation measurements was conducted with a Gamry Interface 1010 E. A current density of 0.05 mA cm^{-2} (C/20) in the potential range of 4.3 V and 2.7 V (vs. Li/Li^{+}) was applied. Electrochemical impedance spectroscopy (EIS) was performed via the same equipment.

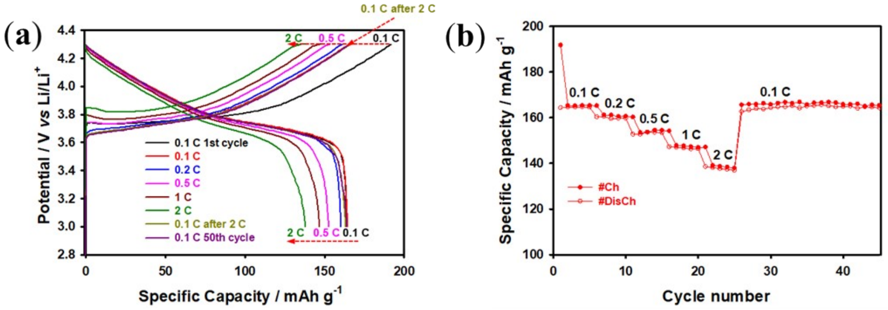

Figure S9. *(a) Rate capabilities and (b) voltage curves of the NCM622 electrode tested in the liquid electrolyte of 1 M* $LiPF_6$ *in EC DEC (1:1 v/v) in the potential range of 3.0−4.3 V (vs.* Li/Li^+*) at various current densities at room temperature.*

Electrochemical evaluation: The NCM cathodes were prepared by blending the obtained powder ($LiNi_{0.6}Co_{0.2}Mn_{0.2}O_2$, provided by Umicore) (92 wt%), polyvinylidene fluoride (Sigma-Aldrich) binder (4 wt%), and carbon black (Super C65, Imerys) conductor (4 wt%) in N-methyl pyrrolidone (NMP, Sigma-Aldrich) via an automatic mixing machine (THINKY MIXER, ARE-250) to obtain a uniformly mixed slurry and cast onto aluminum foil and dried at 120°C for 10 min to eliminate the NMP solvent; the electrode sheets were pressed to ensure interparticle contact and reduce the porosity of the electrode, and then dried at 120°C for overnight in a vacuum oven. The active material of NCM cathodes as a working electrode, Li-metal foil as a counter electrode, and polypropylene as the separator (Celgard 2500) were chosen as the conventional liquid electrolyte of 1 M $LiPF_6$ in EC DEC 1/1 v/v (Aldrich). The charge–discharge tests of NCM cathodes/Li cells were conducted using CR2016 coin-type cells fabricated in an argon-filled glove box. The electrochemical tests were performed at room temperature. The cycling performance was investigated by a MACCOR tester battery cycler in a potential range of 3.0−4.3 V at different C-rates (0.05 C, 0.1 C, 0.2 C, and 0.5 C) and applied to cells to evaluate C-rate performance.